

## Laser Techniques in High-Pressure Geophysics

R. J. HEMLEY, P. M. BELL, H. K. MAO

---

**Laser techniques in conjunction with the diamond-anvil cell can be used to study high-pressure properties of materials important to a wide range of problems in earth and planetary science. Spontaneous Raman scattering of crystalline and amorphous solids at high pressure demonstrates that dramatic changes in structure and bonding occur on compression. High-pressure Brillouin scattering is sensitive to the pressure variations of single-crystal elastic moduli and acoustic velocities. Laser heating techniques with the diamond-anvil cell can be used to study phase transitions, including melting, under deep-earth conditions. Finally, laser-induced ruby fluorescence has been essential for the development of techniques for generating the maximum pressures now possible with the diamond-anvil cell, and currently provides a calibrated in situ measure of pressure well above 100 gigapascals.**

---

**T**HE ORIGINS OF MANY GEOPHYSICAL PHENOMENA observed from our vantage point at the surface of Earth are controlled by forces deep within the planet. Such phenomena—including ocean-floor spreading and continental drift, changes in Earth's magnetic field, deep-focus earthquakes, and regional volcanism—are in turn determined, at least in part, by the properties of the materials that compose Earth's interior. With increasing depth, rocks and fluids are subjected to increasing pressures and temperatures; at the center of the planet the pressures are believed to be close to 3.5 million atmospheres (~350 GPa) and temperatures are perhaps in the neighborhood of 7000 K. The properties of these materials under such extreme conditions are therefore difficult to determine from studies of rocks and fluids sampled at the surface. It has been established experimentally, for example, that densities, crystal structures, elasticity, and thermodynamic properties of minerals below Earth's crust differ markedly in general from those properties measured under ambient pressures and temperatures at the surface.

The fundamental properties of solids and liquids under conditions of extreme pressure and temperature are thus central to our understanding of processes within Earth and other planets (1, 2). An important source of information on properties such as structure and bonding, equations of state, elasticity, and melting under these conditions derives from the application of laser techniques to laboratory studies of samples held under conditions that simulate those found within planetary interiors. The high pressures and temperatures that exist throughout Earth's interior can now be simulated statically in the laboratory by the use of techniques based on the diamond-anvil cell. Moreover, these techniques provide the means with which to make a variety of useful measurements under static high-pressure conditions (3, 4). Optical studies with visible wavelength lasers represent one class of techniques that have been

particularly successful in recent years. This success derives from the fact that the diamond anvils are transparent to visible radiation and, depending on the types of diamonds used, transparent to much of the ultraviolet and infrared spectrum as well (3).

In the past several years the application of laser techniques and diamond-anvil methods to experimental geophysics has advanced as a result of important developments in both high-pressure and optical instrumentation. Ultrahigh pressures well into the 100-GPa range have been attained, and the quality of pressure distribution generated at high pressure has been improved by the use of gas media. On the other hand, micro-focusing and optical sampling techniques have been improved, and more sensitive detection instrumentation has been developed to measure weak signals from small samples under pressure. In this article we highlight these developments by focusing on four experimental techniques that have provided in situ high-pressure measurements useful to geophysics: Raman and Brillouin scattering of minerals and condensed gases and liquids, laser heating of high-pressure phases in the diamond cell, and luminescence spectroscopy of ruby at high pressure.

### Raman Scattering

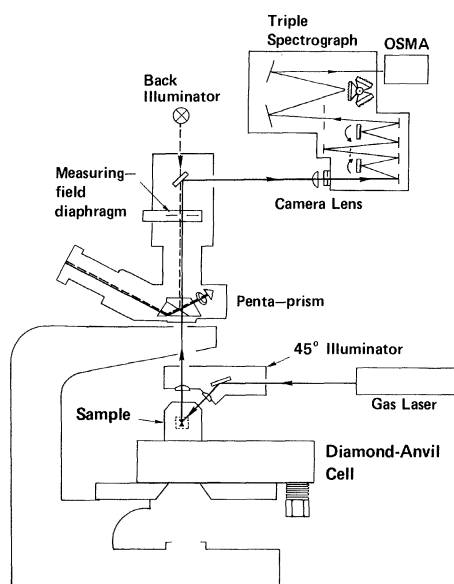
It has long been known that the structure of minerals (such as silicates) can be altered under pressure in a variety of ways to accommodate a more efficient packing of ions. Pressure-induced phase transformations in these materials, in fact, may be responsible for structural features of Earth's interior on a global scale. The question of how minerals compress and the details of high-pressure phase transitions, including the thermodynamic properties and mechanisms on an atomic scale, are thus of fundamental interest. Vibrational spectroscopy of solids pressurized in a diamond-anvil cell is a useful probe of structures and phase transitions at high pressure. In particular, high-pressure laser Raman scattering spectroscopy (Figs. 1 and 2) has emerged as a powerful tool for studies into the 100-GPa range, which covers the range of pressures found within Earth's crust and mantle. The application of pressure provides an important extension of conventional laser Raman studies of earth materials under ambient conditions (5, 6). Along with infrared absorption spectroscopy, this technique serves as a useful complement to high-pressure x-ray diffraction methods (4). The very high pressures possible for these measurements derive from the fact that very small samples (dimensions less than 10  $\mu\text{m}$ ) can be probed. Moreover, single crystals can be preserved with gas pressure-transmitting media to very high pressures (>50 GPa). These pressures, for example, are above the current range of single-crystal diffraction techniques ( $\approx 10$  GPa).

This technique was used in a recent study of the pressure

---

The authors are staff scientists at the Geophysical Laboratory, Carnegie Institution of Washington, Washington, DC 20008.

**Fig. 1.** Schematic diagram for the high-pressure optical studies with the diamond-anvil cell (7). The system is built around a Leitz-Ortholux-I microscope equipped with a variable diaphragm for imaging excitation volumes of dimensions as small as 1  $\mu\text{m}$ . The microscope also uses a penta-prism for simultaneous viewing of the sample, diaphragm, and backlighted spectrometer slits. Excitation is provided typically by continuous wave  $\text{Ar}^+$  and  $\text{Kr}^+$  laser. The laser beam is focused to a beam waist of  $\sim 3 \mu\text{m}$  with a microscope objective (Leitz UM or UT series) mounted within either of two beam-steering attachments on the microscope. This figure shows the attachment that provides a  $\sim 45^\circ$  angle of excitation with respect to the load axis of diamond, thus giving a  $\sim 135^\circ$  scattering configuration. A second attachment provides vertical illumination of the sample ( $180^\circ$  scattering). The  $45^\circ$  design is important for optical studies with diamond-anvil cells because spurious interference due to Raman scattering and possible fluorescence from the diamond anvils along the laser path can be significantly reduced. The scattered light is imaged through the microscope and focused on the slits of the spectrometer with a Micro-Nikkor camera lens. The light is dispersed with a triple spectrograph (Spex 1877) and detected with an optical scanning multichannel analyzer (OSMA). The spectrograph consists of a 0.22-m double-stage system and 0.6-m single-stage system. Typically, the spectra were measured with the entrance slits of the spectrograph set at 50 to 100  $\mu\text{m}$ , for a resolution of 5 to 10  $\text{cm}^{-1}$ . The experiments are performed with a diamond-anvil high-pressure cell based on the Mao-Bell design (4). A detail of the diamond-anvil cell shown in the figure [MBC-L2 type (4)] appears in Fig. 2.



dependence of Raman spectra of the crystalline polymorphs of  $\text{SiO}_2$  (7). The spectra (Fig. 3, left) showed that below 30 GPa pressure affects the structure of these minerals by bending the linkages between  $\text{SiO}_4$  tetrahedra. Above 30 to 35 GPa an interesting pressure-induced transition to a glassy state was observed on room-temperature compression of quartz and coesite. This novel transition is important for understanding both the intrinsic stability of crystal structures under compression and the mechanism of glass formation from crystalline silicates in meteorite impact events. In addition, the high-pressure measurements indicate that a low-frequency vibrational mode in both stishovite and coesite softens (decreases in frequency) under pressure. This soft-mode behavior indicates that the structures weaken with respect to these vibrational coordinates, thereby providing a possible mechanism for observed and predicted high-pressure phase transitions in these polymorphs (Fig. 3, left).

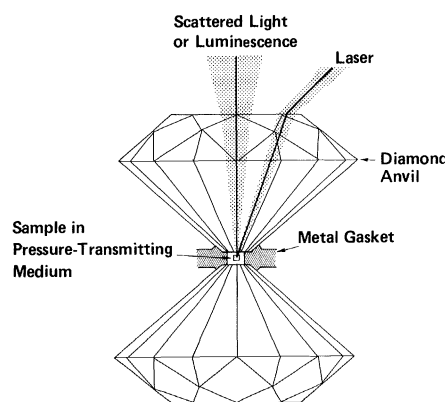
The study of silicate glasses at high pressure represents an important petrologic and geophysical application of high-pressure Raman spectroscopy. There has been a great deal of interest during the last decade in the use of Raman scattering to obtain structural information on silicate glasses for the purpose of understanding the properties of magmas at high temperatures and pressures (8). In many of these studies glasses have been quenched from melts at high pressure and probed under room conditions. Whether the properties of the quenched glasses are similar to those of the melts or glasses at high pressure and temperature has remained an unanswered question, principally because it was not possible to obtain reliable in situ measurements under high-pressure conditions. In the

case of Raman spectroscopy, the problem arises from the low scattering cross section of glasses in comparison to that of crystals. Recent applications of Raman scattering of silicate glasses at high pressure have revealed part of this answer: for a number of silicate glasses the effect of pressure on the structure can be quite large, even at room temperature. Moreover, these structural changes can also be reversible, and hence nonquenchable. Thus, in situ high-pressure measurements are necessary to observe them.

A particularly striking example of this behavior occurs in the Raman spectrum of  $\text{SiO}_2$  glass (9). It has been known for years that silica glass has a number of anomalous high-pressure properties, including a compressibility that increases with pressure and the formation of an irreversibly compacted state at very high pressures ( $>10$  GPa). Very little is known about the structure of the material as a function of pressure, however. With a recently developed optical system (Fig. 1), Raman spectra of  $\text{SiO}_2$  have been obtained as a function of pressure under quasi-hydrostatic conditions. The in situ high-pressure Raman spectra show a marked narrowing of the strong, diffuse peak of the glass when subjected to 8-GPa pressure (Fig. 3, right). At higher pressure the bands begin to weaken and broaden such that by 30 GPa all features in the spectrum are virtually lost. This behavior indicates that a significant increase in intermediate-range order occurs under initial compression. Analysis of the spectra further suggests that a shift in the width and peak of distribution of intertetrahedral ( $\text{Si-O-Si}$ ) angles in the structure at 8 GPa. This behavior is observed in other silicate glasses under pressure in the 10-GPa range. At higher pressures, silica glass becomes densified with rearrangements of the  $\text{SiO}_4$  tetrahedra in compacted configurations such as small, interconnected ring structures (7, 9).

Another class of materials that has been studied successfully with high-pressure Raman scattering includes condensed gases and liquids. Hydrogen is the most abundant element in the universe and the principal constituent of the giant planets. The behavior of hydrogen in the 100-GPa pressure range has been of interest for a number of years, both from a fundamental point of view and for making models of the interiors of these planets (2). Raman spectroscopy has provided the most successful probe of the structure of compressed hydrogen at ultrahigh pressures. In the first high-pressure Raman studies in the gigapascal range the H-H stretching

**Fig. 2.** Detail of the sample probed by the laser while under pressure in the diamond-anvil cell. Brilliant-cut, gem-quality type I and type II diamonds are used both as pressure anvils and as windows on the sample. Type II diamonds are preferred for optical measurements because of a reduction of both fluorescence and Raman scattering from defects in the diamond. The high-pressure chamber typically consists of a 30- to 300- $\mu\text{m}$  hole drilled in the metal gasket. Small chips of ruby are placed in the sample chamber for in situ pressure determinations. Samples are loaded with a transmitting medium, consisting of a condensed gas or fluid. Rare gases such as argon and neon have been shown to produce quasi-hydrostatic conditions to pressures above 80 GPa and are particularly useful because these materials lack a first-order Raman spectrum in the solid state and hence do not contribute to the background signal. Gas media are loaded in the high-pressure cell either cryogenically or by prepressurizing the gas at room temperature in a high-pressure apparatus.



mode, or vibron, in the solid was measured, and this measurement indicated that a weakening of intramolecular bond occurs above 30 GPa (10, 11). In more recent studies (12), the solid has been pressurized to 147 GPa. Raman spectra indicate that the solid remains molecular, as evidenced by the detection of a well-defined vibron band, at these pressures (Fig. 4, top). A significant drop in the frequency of the band occurs above 30 GPa, however, which suggests a continued weakening of the H–H bond (Fig. 4, bottom). Moreover, an anomalously large isotope effect in the pressure dependence of the frequency was observed, which has recently been explained as resulting from the large zero-point motion in hydrogen relative to deuterium (13). In an interesting application of Raman spectroscopy of hydrogen at lower pressures, Loubeyre *et al.* (14) determined the phase diagram of fluid H<sub>2</sub> and He, an important chemical system for interior models of the giant planets (2).

Spectroscopic studies of other diatomic molecules at high pressure can give us some insight into the behavior of hydrogen. Raman spectra of solid N<sub>2</sub> pressurized to 140 GPa (15) and 170 GPa (16) indicate a weakening of the N≡N bond on compression but also show evidence for several phase transitions in the molecular solid. High-pressure Raman studies at both high and low temperatures have been useful for the determination of the phase diagram of solid molecular nitrogen at lower pressures (17). The results of these static high-pressure investigations can be compared with recent spectroscopic measurements of materials under dynamic compression (that is, shock wave) conditions. Measurements of N<sub>2</sub> spectra at high temperatures and pressures (4400 K and 34 GPa) have been performed recently by dynamic compression techniques (18). In this experiment, coherent anti-Stokes Raman scattering (CARS) spectroscopy was performed on fluid N<sub>2</sub> and shows the effect of very high temperatures on the frequency of the N≡N vibron on compression.

Finally, we note that the behavior of H<sub>2</sub>O at high pressure has

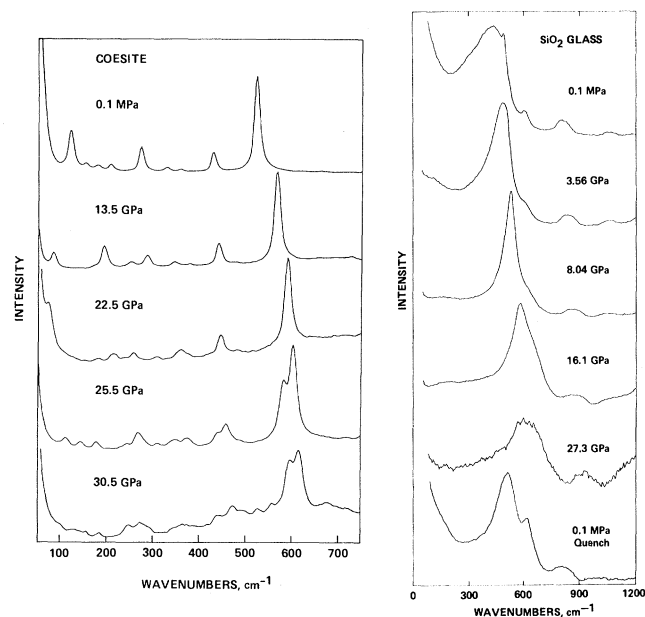


**Fig. 3.** Pressure dependence of the Raman spectrum of SiO<sub>2</sub> phases with an argon pressure-transmitting medium. Samples of 10 to 50 μm in length and 10 to 40 μm in thickness were used. Care was taken to prevent bridging of the sample between the diamond anvils. (Left) Coesite, a high-pressure polymorph. Note the change in the spectrum between 22 and 25 GPa, indicative of a phase transition, and the increase in diffuse scatter in the highest pressure spectrum due to pressure-induced amorphization [reprinted from (7) with permission, copyright Terra Scientific]. (Right) SiO<sub>2</sub> glass (vitreous silica) [reprinted from (9) with permission, copyright the American Physical Society].

been of broad interest as this material is believed to be a major constituent of the interiors of the outer planets and planetary satellites (2). Walrafen *et al.* (19) have obtained Raman spectra of the H<sub>2</sub>O (ice-VII) to 36.0 GPa which indicate a lengthening of the molecular O–H bond on compression. On the basis of Raman spectra, Hirsch and Holzapfel (20) have observed a discontinuity in the Raman spectrum of H<sub>2</sub>O at 100 K between 30 and 40 GPa, and have suggested that this is indicative of the transition to the ice-X phase in which hydrogen bonding is effectively lost. In a set of dynamic compression experiments, Holmes *et al.* (21) succeeded in measuring the Raman spectrum of fluid H<sub>2</sub>O to 26 GPa and 1700 K. These data indicate the breakdown of the hydrogen-bonded structure above approximately 12 GPa. The principal conclusion of these studies is that H<sub>2</sub>O at high pressures (and temperatures) is characterized by significantly different bonding, and hence markedly different physical properties, in comparison to liquid and solid H<sub>2</sub>O at near-ambient conditions.

## Brillouin Scattering

The interpretation of seismic data in terms of component rocks and minerals requires information on the elasticity of minerals at

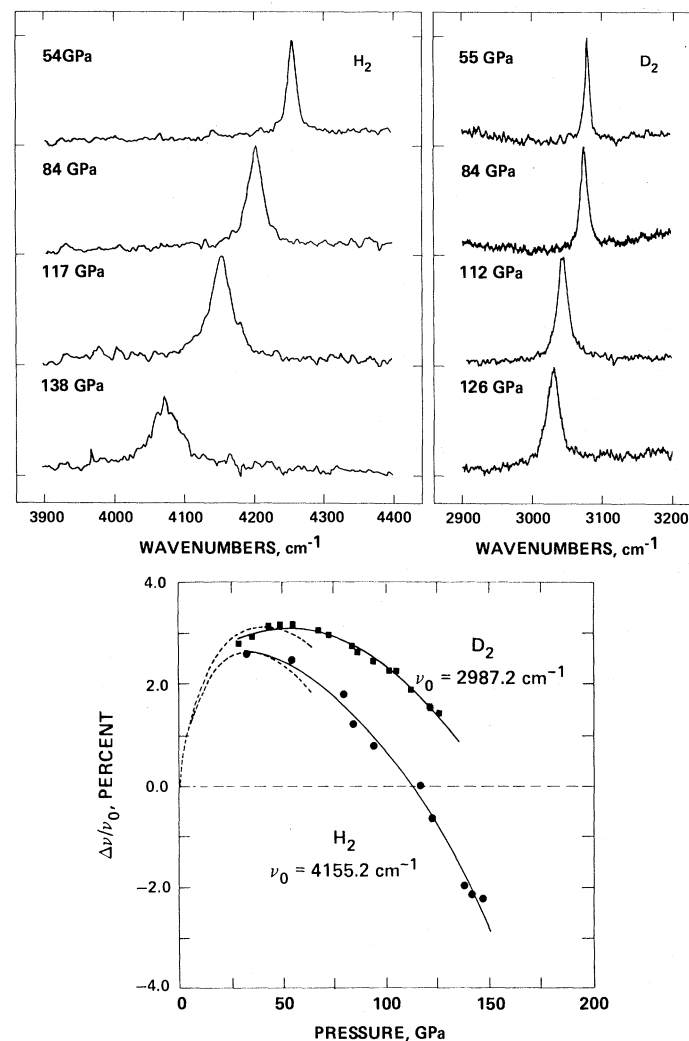


**Fig. 4.** (Top) Raman spectra of solid normal hydrogen and deuterium at high pressure [reprinted from (12) with permission, copyright the American Physical Society]. (Bottom) Pressure dependence of the frequency of the intramolecular stretching mode in solid hydrogen and deuterium. The zero-pressure (low-temperature) reference frequencies are indicated. The dashed lines are fits to the earlier data of Sharma *et al.* (10).

high pressure (*1*). From data on elasticity as a function of pressure, equations of state can be determined. Information on elasticity also provides a microscopic view of the manner in which crystals respond to applied stress. The development of techniques for the measurement of elasticity of materials at high pressures is thus exceedingly useful in both solid-earth geophysics and mineralogy. One such technique is high-pressure Brillouin scattering spectroscopy, which involves the measurement of Doppler-shifted light that is inelastically scattered by acoustic phonons in a condensed medium. Acoustic velocities as a function of propagation direction are measured, from which elastic moduli can be calculated. The Brillouin scattering technique is readily combined with the diamond-anvil cell for elasticity studies on materials under very high pressures (Fig. 5). A

visible wavelength laser provides the excitation, and a Fabry-Perot interferometer detects the scattered light. Because of the small sample size and the effects of spurious scattering from the cell, considerable effort must be expended to resolve the weak Brillouin components from the much stronger elastic peak. This is accomplished by multipassing the laser through the interferometer (*22*).

A number of minerals important to geophysics have been studied by Brillouin scattering techniques under ambient conditions, principally by Weidner and colleagues (*23*). These phases include high-pressure polymorphs of  $\text{SiO}_2$  (coesite and stishovite),  $\text{Mg}_2\text{SiO}_4$  ( $\beta$ - and  $\gamma$ -phases),  $\text{MgSiO}_3$  (ilmenite structure), and silicate garnets (*23*). The most complete high-pressure Brillouin scattering study of a silicate mineral is that of forsterite ( $\alpha$ - $\text{Mg}_2\text{SiO}_4$ ) by Bassett *et al.* (*24*). Previous measurements of the single-crystal moduli at high pressure were made by ultrasonic techniques, which, although more precise, were limited to 1 GPa and below. Bassett *et al.* measured the elastic moduli to 4.0 GPa (Fig. 6) and from the extended pressure range were able to estimate the sign of the second pressure derivatives of the single-crystal moduli. The data provide evidence for a weakening of the olivine structure with respect to shear stress on compression. These investigators proposed that this weakening of the structure may relate to the mechanism of the phase transition to the denser  $\beta$ - and  $\gamma$ -phases at  $\sim 14$  GPa, which is believed to be responsible for the discontinuity observed in seismic waves at 400-km depth in the mantle (*1*).

The determination of elastic moduli of condensed gases, such as hydrogen and deuterium, represents another application of high-pressure Brillouin scattering. These measurements are important for the calculation of high-pressure equations of state used in planetary modeling studies (*2*). Room-temperature Brillouin scattering spectra have been obtained for normal (para and ortho) fluid  $\text{H}_2$  and  $\text{D}_2$  pressurized to the freezing point at 5.4 GPa and for the solid phases from 5.4 to 20 GPa (*25, 26*). These data yielded the pressure dependence of the longitudinal and transverse sound velocities, from which the bulk modulus as a function of pressure and the pressure-volume equation of state were calculated. The equation of state of the solid in the lower pressure regime is in good agreement with that determined directly by single-crystal x-ray diffraction measurements (*27*), although at higher pressure the Brillouin scattering equation of state is somewhat softer. Recently, the technique of high-pressure Brillouin scattering has been applied to  $\text{H}_2\text{O}$ -ice, where evidence is found for a phase transition at  $\sim 46$  GPa (*28*), which is close to the pressure at which a transformation has been observed in the Raman measurements (*20*). Information on the pressure dependence of the elastic constants of solidified rare gases

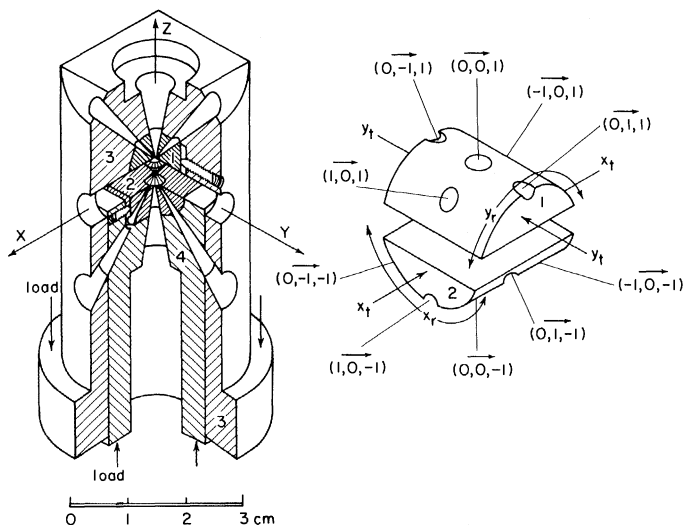
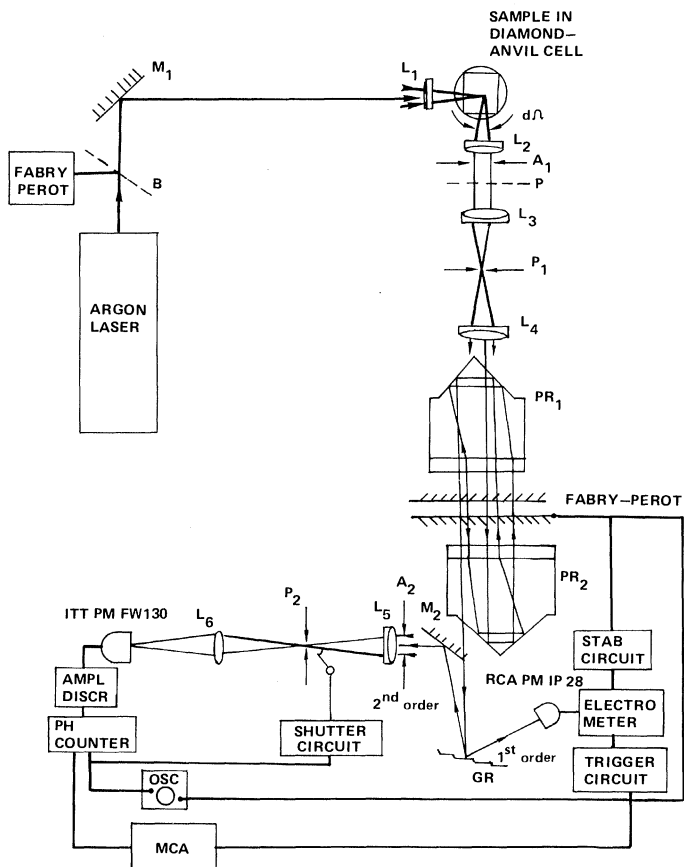


**Fig. 5. (Top)** Schematic diagram of the Brillouin scattering experiment for high-pressure elasticity measurements. Excitation is provided by light from an  $\text{Ar}^+$  laser, which is focused on the sample after passing through a beam splitter (B), mirror ( $M_1$ ), and lens ( $L_1$ ). The scattered light is collected by a lens ( $L_2$ ), polarized with a polarizer (P), and spatially filtered with an aperture ( $A_1$ ). The light is then imaged on a pinhole ( $P_1$ ) and directed into the Fabry-Perot interferometer with lenses  $L_3$  and  $L_4$ . A pair of prisms ( $PR_1$  and  $PR_2$ ) is aligned for five passes through the interferometer. Extrinsic scattered light and fluorescence by a grating (GR), lenses ( $L_5$  and  $L_6$ ), and apertures ( $A_2$ ), is detected by a photomultiplier tube (ITT PM FW130), processed by a photon counter and displayed on an oscilloscope (OSC), and stored in a multichannel analyzer (MCA). Weak first-order diffraction from the grating is detected by a second photomultiplier (RCA PM IP28), which is used to stabilize the interferometer and to trigger the sweep of the multichannel analyzer. **(Bottom)** Design of the diamond-anvil cell used for high-pressure Brillouin scattering measurements. A sectional view of the piston-cylinder portion of the cell is shown on the left. The exploded view on the right shows the ports and the geometric direction indices in the tungsten carbide rockers that support the diamond anvils (parts 1 and 2 on left). This cell was used for Brillouin measurements on condensed hydrogen and deuterium (*25, 26*).

at very high pressures has also been obtained in recent work with these techniques (29).

## Laser Heating

Both high temperatures and high pressure are found within Earth. The geotherm of Earth is such that the pressure and temperatures at the core-mantle boundary, at a depth of  $\sim 2900$  km, are estimated to be 130 GPa and approaching 4000 K, respectively (30). The generation of extreme pressures and temperatures, together with accurate measurements of mantle and core materials under these conditions, is thus an important thrust of experimental geophysics. The combination of high temperature and high pressure can be generated under dynamic compression (shock wave) techniques for a variety of materials, as discussed above. The creation of these conditions in static experiments represents an alternative strategy, and one with potentially more flexibility in terms of control of temperature and pressure.

These conditions have been realized in the laboratory by heating samples at high pressure in a diamond-anvil cell. In the lower temperature domain below  $\sim 1200$  K, the anvils can be heated resistively (3, 4). To attain higher temperatures, samples in the diamond-anvil cell can be heated with an intense laser source. The most successful of the latter techniques uses a continuous-wave Nd-

YAG (yttrium-aluminum-garnet) laser (wavelength  $\lambda = 1.064 \mu\text{m}$ ), which is focused with micro-laser optics on a sample in the cell (31). The diamond anvils are transparent to radiation at this wavelength, yet many minerals absorb near-infrared radiation and can be heated to temperatures in excess of those of the core with a sufficiently powerful laser. The coupling of the near-infrared radiation is particularly strong for iron-bearing phases, important for simulations of the mantle and core. To heat samples that may be transparent at this wavelength, strongly absorbing material such as graphite or platinum black may be mixed in with the sample under study. Typically, the temperature of the sample is determined by optical pyrometry.

The earliest investigations of minerals heated by laser at high pressures in a diamond-anvil cell were important synthesis studies that were instrumental in detailing the rich chemistry of silicates at pressures and temperatures of Earth's transition zone and lower mantle (1). High-pressure silicate phases having the spinel, garnet, ilmenite, and perovskite structures were synthesized. Perhaps most significant was the synthesis and identification of the perovskite phase of  $\text{MgSiO}_3$  by Liu in 1974 (32). This was followed by structural and equation of state studies of laser-synthesized  $\text{MgSiO}_3$ -perovskite by x-ray diffraction (33). Later studies established phase relations for much of the  $\text{MgO-CaO-FeO-Al}_2\text{O}_3\text{-SiO}_2$  system in the  $1000^\circ\text{C}$  and 50-GPa range (34, 35). Recently, Knittle and Jeanloz (36) have shown by x-ray diffraction that laser-heated

**Fig. 6. (Top)** A typical sample configuration for Brillouin scattering measurements. The high-pressure measurements were performed on the sample in a 4:1 methanol-ethanol pressure medium. The letters a, b, and c refer to the crystallographic axes of forsterite, which is orthorhombic. The letter q represents the propagation direction of the thermal phonon. This configuration yields the spectrum shown in Fig. 5. **(Bottom)** The Brillouin spectra of forsterite oriented as in (top). The electric vector of the incident light was horizontal for both spectra. The electric vector of the scattered light was vertical for the upper spectrum (HV) and horizontal for the lower spectrum (HH). The central large peak is the unshifted laser frequency due to Rayleigh scattering. The TA (LA) peaks are due to light scattered by transverse (longitudinal) acoustic phonons. The values for the elastic constants  $C_{66}$  and  $C_{11}$  can be calculated from the upper and lower spectra, respectively [reprinted from (24) with permission, copyright Center for Academic Publications Japan].

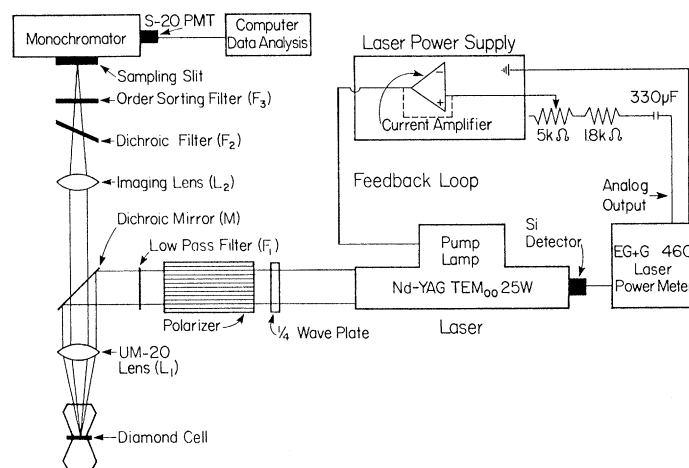
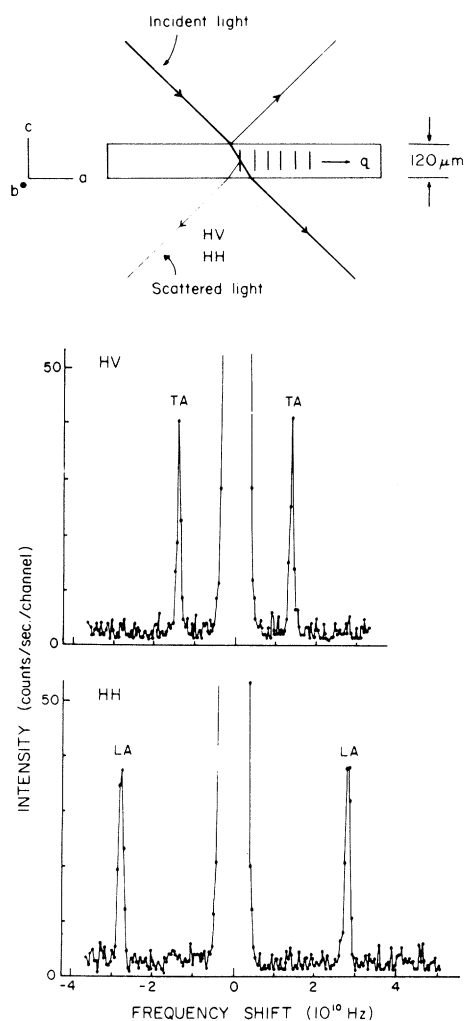
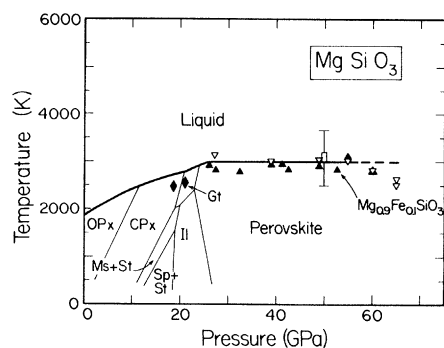


**Fig. 7.** Schematic diagram for laser heating and temperature measurement of samples in a diamond-anvil cell. A Quantronix model 117 actively stabilized Nd-YAG laser with a maximum output of 25 watts at  $\lambda = 1.064 \mu\text{m}$  (cw TEM<sub>00</sub> mode) is used. The TEM<sub>00</sub> mode gives a temperature distribution in the sample which is approximately radially symmetric. The power at the sample can be controlled by passing the beam through a  $\lambda/4$  plate to rotate the plane of polarization and then through a Brewster polarizer. This feature serves as an optical-feedback isolation system to minimize instabilities of the laser. A low-pass filter (F<sub>1</sub>) prevents visible and near-infrared light from the pump lamp from reaching the sample and spectroradiometer. The laser beam is reflected off a dichroic mirror (M), which is designed to reflect infrared and transmit visible radiation. The beam is then focused onto the sample with a Leitz UM-20 lens (L<sub>1</sub>). The focal spot is between about 10 and 30  $\mu\text{m}$  in radius. The thermal radiation collected from the sample by the objective lens (L<sub>1</sub>) is focused with a biconvex lens (L<sub>2</sub>) onto the entrance slit of the monochromator. The dichroic filter (F<sub>2</sub>) filters out any stray laser radiation. The image of the entrance slit is focused onto the exit slit by a concave holographic grating; an order-sorting filter (F<sub>3</sub>) prevents the overlap of different orders of the dispersed spectrum. A slit width of 0.83 mm results in a spectral resolution of 10 nm. Detection is provided by an S-20 type photomultiplier tube (PMT) or silicon detector [reprinted from (38) with permission, copyright Terra Scientific].

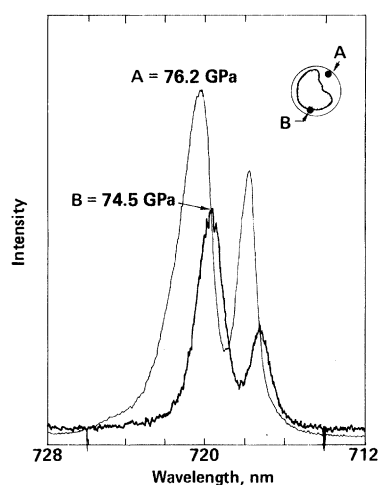
**Fig. 8.** Melting curve of  $\text{Mg}_{0.9}\text{Fe}_{0.1}\text{SiO}_3$  perovskite determined by laser heating diamond-anvil techniques. The solid diamonds and the solid triangles are the highest peak temperature observed before the appearance of glass produced by quenching the melt. The open triangles are the lowest peak temperatures observed when glass is present. The diamond symbols represent the experimental determinations of the melting of  $\text{Mg}_{0.9}\text{Fe}_{0.1}\text{SiO}_3$  below 22 GPa. Above 22 GPa the perovskite structure is the stable solid phase. The open box (at 50 GPa) with an error bar represents a direct determination of the temperature of the liquid-crystal interface. The stability fields of the solid phases at lower temperatures and pressures are indicated and labeled as follows: OPx, orthopyroxene; CPx, clinopyroxene; Ms, magnesio-wustite; St, stishovite; Sp, spinel; Il, ilmenite; and Gt, garnet [reprinted from (39) with permission, copyright the American Geophysical Union].



$\text{Mg}_{0.9}\text{Fe}_{0.1}\text{SiO}_3$  remains in a perovskite-like structure to nearly the maximum pressure found in the lower mantle. On the basis of the large volume of lower mantle, they postulate that  $\text{Mg}_{0.9}\text{Fe}_{0.1}\text{SiO}_3$ -perovskite may be the most abundant mineral in Earth. The room-temperature pressure-volume relations of the laser-synthesized  $\text{MgSiO}_3$ -perovskite were also obtained to over 100 GPa (36), and the results were consistent with the earlier equation of state determined from low-pressure data (33).

Recently, efforts have been made to improve the accuracy of the temperature measurement in laser-heating experiments. Single-channel photomultiplier tube systems have been replaced by fixed grating spectrographs equipped with multichannel analyzers, which permit reduced measurement time and potentially better accuracy in the determination of temperature fluctuations in the sample (37). Jeanloz and Heinz (38) have expended considerable effort to characterize the thermal state of a sample in a laser-heated diamond-anvil cell and have developed techniques for measuring temperature gradients across the heated region of the sample (Fig. 7). This development is particularly significant because temperature gradients can be large as a result of the high thermal conductivity of the diamond anvils in contact with the laser-heated sample.

**Fig. 9. (Left)** Luminescence spectra of ruby in a solid argon medium at a nominal pressure of 75 GPa. The inset sketch shows the position of two ruby grains designated A and B within the high-pressure chamber of the diamond-anvil cell. The central, hatched region indicates the position of the powdered copper sample probed by x-ray diffraction [reprinted from (44) with permission, copyright American Geophysical Union]. **(Right)** Calibration of the wavelength of the ruby  $R_1$  band (the more intense peak in the spectrum) as a function of pressure,  $P$ . Filled circles are data with powdered copper sample (44) and filled triangles are data with powdered silver sample (45). The line represents a fit to the data with the following formula,  $P = a/b[(1 + (\Delta\lambda/\lambda_0))^b - 1]$ , with  $a = 1904$  GPa,  $b = 7.665$ , and  $\lambda_0 = 694.2$  nm, which represents the quasi-hydrostatic ruby pressure gauge.

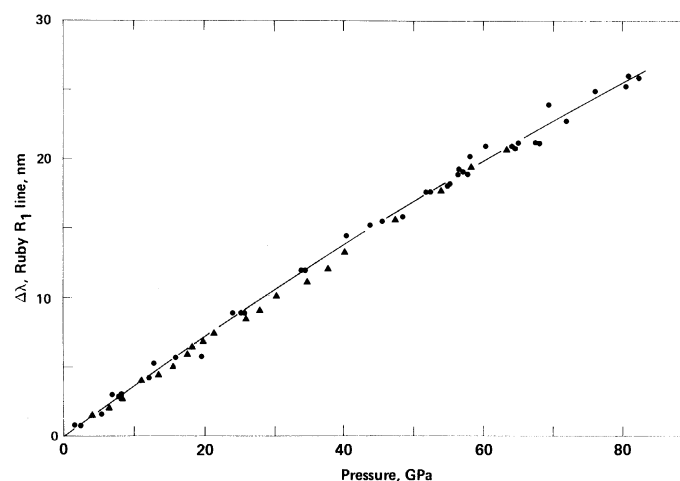


With this technique, the first data on melting curves of several important high-pressure phases at lower mantle pressures have been determined by this group (39, 40). Heinz and Jeanloz (39) have measured the melting curve of  $\text{Mg}_{0.9}\text{Fe}_{0.1}\text{SiO}_3$ -perovskite to 60 GPa. They found that the perovskite melts at  $2900 \pm 300$  K above 25 GPa and that the melting curve is, within the stated error, independent of pressure to 60 GPa [Fig. 8; see also (30)]. This result has important implications for the relative densities of coexisting crystals and melts at these pressures and temperatures within Earth. Williams *et al.* (40) have measured the melting curve of iron to 100 GPa. Extrapolation of this curve to core pressures (130 to 370 GPa) appears to be consistent with shock-wave results and gives, after an analysis of the effect of alloying in the core, an estimated temperature at the center of Earth of  $6900 \pm 1000$  K. This temperature is significantly higher than previous estimates based on much larger extrapolations of experimental data.

## Ruby Fluorescence

The ultrahigh pressures generated within a diamond-anvil cell must be determined by in situ methods. An important and widely used in situ technique for pressure determinations is the ruby fluorescence method, which involves measuring the pressure shift of the  $R_1$  ( ${}^2E_1 \rightarrow {}^4A_2$ ) luminescence band of ruby ( $\text{Al}_2\text{O}_3$  with  $\text{Cr}^{+3}$  impurity), which has a strong pressure dependence. The  $R_1$  band is relatively sharp and intense, particularly at low pressure where the quantum yield is  $\approx 1$  and can be excited with commercially available lasers (He-Cd at 442 nm and  $\text{Ar}^+$  at 458 to 488 nm, for example). Considerable work has gone into the calibration of the ruby  $R_1$  pressure scale. As a result of the pioneering work performed in part at the National Bureau of Standards in the early 1970s, the scale was calibrated to 30 GPa (41). In 1978 the pressure scale was extended to 100 GPa by calibrating the wavelength shift of the  $R_1$  band against molar volume of metal standards by x-ray diffraction (42). The pressure was calculated from the room-temperature pressure-volume isotherm of the metal determined by shock-wave techniques.

The calibration of the ruby scale has been extended in recent studies. In the first, the earlier calibration was continued to 180 GPa under nonhydrostatic conditions with samples consisting of ruby and either gold or copper (43). The pressure shift of the ruby bands against the equations of state of copper and gold has been calibrated



to 80 GPa in an argon medium, which provides a quasi-hydrostatic environment at very high pressures (44, 45). The lack of broadening of the  $R_1$  (and  $R_2$ ) bands at high pressure with the use of such media results in greater precision in the measurement of pressure (Fig. 9). This pressure scale gives higher pressures for a given wavelength shift than the earlier scales, particularly above 100 GPa. The quasi-hydrostatic pressure scale is of obvious relevance to the spectroscopic studies of minerals and gases described above because the use of similar media in these experiments results in similar (and in many cases identical) stress conditions at high pressure. The pressure dependence of secondary spectral bands in the region of the  $R_1$  and  $R_2$  bands has also been examined in quasi-hydrostatic compression experiments and shown to not interfere with the primary luminescence bands to above 100 GPa (46). The measurement of the pressure distributions in the diamond-anvil cell with the ruby technique has been applied to the study of the yield strength of materials under pressure (47, 48). This work is important both for the development of ultrahigh-pressure techniques, by detailed measurements of stress conditions in the diamond-anvil cell, and for the determination of the yield strength of mineral samples in the cell under mantle and core pressures.

During the past 2 years, efforts to generate maximum static pressures with the diamond-anvil cell have resulted in ultrahigh-pressures that are beyond the range of the current ruby calibration. Initial studies of ruby fluorescence at higher pressures were complicated by the observation that above  $\sim 200$  GPa the intensity of the ruby fluorescence decreased markedly with increasing pressure (49). In addition, increasing intensity of spurious fluorescence from the strained diamond anvils precluded the measurement of the ruby signal and hence the calculation of pressure. In a series of ultrahigh-pressure experiments with beveled diamonds, pressure gradients given by the ruby scale were carefully measured across the sample under pressure. Extrapolation of the pressure gradients, together with load calculations, indicated peak pressures in excess of 275 GPa were obtained (49). In subsequent work with more sensitive optical instrumentation and a more intense  $\text{Ar}^+$  laser source (Fig. 2), ruby fluorescence at considerably higher pressures could be measured. Recently, pressures of 550 GPa on the extrapolated (nonhydrostatic) ruby pressure scale have been measured at the Geophysical Laboratory (50). Ultrahigh pressures (460 GPa) have also been reported in similar experiments at Lawrence Livermore National Laboratory (51).

## Conclusions and Outlook

Raman scattering spectroscopy can reveal detailed changes in structure and bonding in a variety of earth and planetary materials under geophysically relevant, in situ high-pressure conditions. This development is particularly well illustrated by high-pressure Raman studies of silicate glasses and condensed gases, materials that are difficult to study by other high-pressure techniques such as x-ray diffraction. On the basis of preliminary work at lower pressures, Raman techniques appear to have great potential for in situ phase equilibrium studies of both minerals systems and condensed planetary gases in the 100-GPa range. There have been comparatively few Brillouin scattering studies of minerals at high pressure, but it is expected that the need for accurate interpretation of seismic data in terms of the properties of constituent minerals will promote continued development and application of this technique at mantle pressures. The ruby fluorescence method has been instrumental in the continued development of static ultrahigh-pressure techniques, and remains a viable secondary standard for studies in the 100-GPa pressure range.

Applications of new spectroscopic techniques, such as double resonance, ultrafast kinetics, Fourier-transform Raman, and nonlinear optical methods, are likely prospects in future work on geophysical problems with the diamond-anvil cell. Recent high-pressure studies involving the use of picosecond spectroscopy (52) and hyper-Raman scattering of perovskites (53) may be representative of this trend. Time-resolved studies may permit the detailed investigation of the kinetics of high-pressure phase transitions and the rheology of minerals under in situ deep-earth conditions. Finally, the combination of spectroscopic and x-ray diffraction probes with laser-heating techniques may yield detailed structural information on earth materials at high temperatures and pressures. This information may play an important role in advancing our understanding the connection between atomic-scale properties and global deep-earth processes.

## REFERENCES AND NOTES

1. D. L. Anderson, *Science* **223**, 347 (1984); S. K. Saxena, Ed., *Advances in Physical Geochemistry, Chemistry and Physics of Terrestrial Planets* (Springer-Verlag, New York, 1986), vol. 6.
2. Discussion of the use of high-pressure data in interior models of the gaseous planets is found in: D. J. Stevenson, *Annu. Rev. Earth Planet. Sci.* **10**, 257 (1982); W. B. Hubbard, *Planetary Interiors* (Van Nostrand Reinhold, New York, 1984); and G. H. A. Cole, *Physics of Planetary Interiors* (Hilger, Bristol, Great Britain, 1984).
3. General reviews of the use of diamond-anvil cell techniques can be found in A. J. Jayaraman, *Rev. Mod. Phys.* **55**, 65 (1983); *Rev. Sci. Instrum.* **57**, 1013 (1986).
4. A detailed description of the operation of the megabar-type diamond-anvil cell is described by A. P. Jephcoat, H. K. Mao, P. M. Bell, in *Hydrothermal Experimental Techniques*, H. L. Barnes and G. Ulmer, Eds. (Wiley-Interscience, New York, in press), chap. 19.
5. P. McMillan, in *Microscopic to Macroscopic: Atomic Environments to Mineral Thermodynamics*, vol. 14 of *Reviews in Mineralogy*, S. W. Kieffer and A. Navrotsky, Eds. (Mineralogical Society of America, Washington, DC, 1985), pp. 9–63.
6. S. K. Sharma, J. F. Mammone, M. F. Nicol, *Nature (London)* **292**, 140 (1981); R. J. Hemley, H. K. Mao, E. C. T. Chao, *Phys. Chem. Miner.* **13**, 285 (1986); P. F. McMillan and N. L. Ross, *ibid.* **14**, 225 (1987); P. McMillan and M. Akaogi, *Am. Mineral.* **72**, 361 (1987); Q. C. Williams, R. Jeanloz, P. McMillan, *J. Geophys. Res.*, in press.
7. R. J. Hemley, in *High-Pressure Research in Mineral Physics*, M. H. Manghnani and Y. Syono, Eds. (Terra Scientific, Tokyo, in press).
8. B. O. Mysen, *Annu. Rev. Earth Planet. Sci.* **11**, 75 (1983); P. McMillan, *Am. Mineral.* **69**, 622 (1984).
9. R. J. Hemley, H. K. Mao, P. M. Bell, B. O. Mysen, *Phys. Rev. Lett.* **57**, 747 (1986).
10. S. K. Sharma, H. K. Mao, P. M. Bell, *ibid.* **44**, 886 (1980); *Carnegie Inst. Washington Yearb.* **79**, 358 (1980).
11. R. J. Wijngaarden, A. Lagendijk, I. F. Silvera, *Phys. Rev. B* **26**, 4957 (1982).
12. H. K. Mao, P. M. Bell, R. J. Hemley, *Phys. Rev. Lett.* **55**, 99 (1985).
13. N. W. Ashcroft, *Phys. Chem.*, in press.
14. P. Loubeyre, R. Le Toullec, J. P. Pinceaux, *Phys. Rev. B* **32**, 7611 (1986).
15. R. Reichlin, D. Schiferl, S. Martin, C. Vanderborgh, R. L. Mills, *Phys. Rev. Lett.* **55**, 1464 (1985).
16. P. M. Bell, H. K. Mao, R. J. Hemley, *Physica* **139** and **140B**, 16 (1986); R. J. Hemley, H. K. Mao, P. M. Bell, in preparation.
17. D. Schiferl, S. Buchsbaum, R. L. Mills, *J. Phys. Chem.* **89**, 2324 (1985).
18. S. C. Schmidt, D. S. Moore, M. S. Shaw, *Phys. Rev. B* **35**, 493 (1987).
19. G. E. Walrafen *et al.*, *J. Chem. Phys.* **77**, 2166 (1982).
20. K. R. Hirsch and W. B. Holzapfel, *ibid.* **84**, 2771 (1986).
21. N. C. Holmes, W. J. Nellis, W. B. Graham, G. E. Walrafen, *Phys. Rev. Lett.* **55**, 2433 (1985).
22. J. G. Dil and E. M. Brody, *Phys. Rev. B* **14**, 5218 (1976); C. H. Whitfield, E. M. Brody, W. A. Bassett, *Rev. Sci. Instrum.* **47**, 942 (1976). The design of the Brillouin scattering spectrometer is based on that originally developed by J. R. Sandercock [*Phys. Rev. Lett.* **28**, 237 (1972); *RCA Rev.* **36**, 89 (1975)].
23. D. J. Weidner, J. D. Bass, M. T. Vaughan, in *High-Pressure Research in Geophysics*, S. Akimoto and M. H. Manghnani, Eds. (Kluwer Academic, Norwell, MA, 1982), pp. 125–133. More recent results are summarized by D. J. Weidner, in *Advances in Physical Geochemistry, Chemistry and Physics of Terrestrial Planets*, S. K. Saxena, Ed. (Springer-Verlag, New York, 1986), vol. 6, pp. 251–274; M. T. Vaughan and S. Guggenheim, *J. Geophys. Res.* **91**, 4657 (1986).
24. W. A. Bassett, H. Shimizu, E. M. Brody, in *High-Pressure Research in Geophysics*, S. Akimoto and M. H. Manghnani, Eds. (Kluwer Academic, Norwell, MA, 1982), pp. 115–124.
25. E. M. Brody, H. Shimizu, H. K. Mao, P. M. Bell, W. A. Bassett, *J. Appl. Phys.* **52**, 3583 (1981).
26. H. Shimizu, E. M. Brody, H. K. Mao, P. M. Bell, *Phys. Rev. Lett.* **47**, 128 (1981).
27. R. M. Hazen, H. K. Mao, L. W. Finger, R. J. Hemley, *Phys. Rev. B*, in press.
28. A. Polian and M. Grimsditch, *Phys. Rev. Lett.* **52**, 1312 (1984); A. Polian, J. M. Besson, M. Grimsditch, in *Solid State Physics under Pressure*, S. Minomura, Ed. (Kluwer Academic, Norwell, MA, 1985), pp. 93–98.
29. M. Grimsditch, P. Loubeyre, A. Polian, *Phys. Rev. B* **33**, 7192 (1986); A. Polian and M. Grimsditch, *Europhys. Lett.* **2**, 849 (1986).
30. R. Jeanloz and S. Morris, *Annu. Rev. Earth Planet. Sci.* **14**, 377 (1986).
31. L. Ming and W. A. Bassett, *Rev. Sci. Instrum.* **45**, 1115 (1974).

32. L. G. Liu, *Geophys. Res. Lett.* **1**, 277 (1974).
33. T. Yagi, H. K. Mao, P. M. Bell, *Phys. Chem. Miner.* **3**, 97 (1978); in *Advances in Physical Geochemistry*, S. K. Saxena, Ed. (Springer-Verlag, New York, 1982), vol. 2, pp. 317–325.
34. T. Yagi *et al.*, *Carnegie Inst. Washington Yearb.* **78**, 614 (1979); H. K. Mao, P. M. Bell, T. Yagi, in *High-Pressure Research in Geophysics*, S. Akimoto and M. H. Manghnani, Eds. (Kluwer Academic, Norwell, MA, 1982), pp. 319–325.
35. L. G. Liu, *Phys. Earth Planet. Inter.* **11**, 289 (1976); in *The Earth: Its Origin, Structure, and Evolution*, M. W. McElhinny, Ed. (Academic Press, London, 1979), pp. 177–202.
36. E. Knittle and R. Jeanloz, *Science* **235**, 668 (1987).
37. W. A. Bassett and M. S. Weathers, *Physica* **139** and **140B**, 900 (1986); H. K. Mao and P. M. Bell, in preparation.
38. R. Jeanloz and D. L. Heinz, *J. Phys.* **C8**, 83 (1984); D. L. Heinz and R. Jeanloz, in *High-Pressure Research in Mineral Physics*, M. H. Manghnani and Y. Syono, Eds. (Terra Scientific, Tokyo, in press).
39. D. Heinz and R. Jeanloz, *J. Geophys. Res.*, in press.
40. Q. Williams, R. Jeanloz, J. Bass, B. Svendsen, T. J. Ahrens, *Science* **236**, 181 (1987).
41. R. A. Forman, G. J. Piermarini, J. D. Barnett, S. Block, *ibid.* **176**, 284 (1972); J. D. Barnett, S. Block, G. J. Piermarini, *Rev. Sci. Instrum.* **44**, 1 (1973); G. J. Piermarini, S. Block, J. D. Barnett, R. A. Forman, *J. Appl. Phys.* **46**, 2774 (1975).
42. H. K. Mao, P. M. Bell, J. W. Shaner, D. J. Steinberg, *J. Appl. Phys.* **49**, 3276 (1978).
43. P. M. Bell, J. A. Xu, H. K. Mao, in *Shock Waves in Condensed Matter*, Y. M. Gupta, Ed. (Plenum, New York, 1986), pp. 125–130.
44. H. K. Mao, J. A. Xu, P. M. Bell, *J. Geophys. Res.* **91**, 4673 (1986).
45. G. Zou, P. M. Bell, H. K. Mao, *Carnegie Inst. Washington Yearb.* **81**, 436 (1982).
46. R. J. Hemley, H. K. Mao, P. M. Bell, in preparation. Low-pressure studies of secondary ruby luminescence bands have been described by L. D. Merkle, I. L. Spain, R. C. Powell, *J. Phys. C* **14**, 2027 (1981); Q. Williams and R. Jeanloz, *Phys. Rev. B* **31**, 7449 (1985).
47. H. K. Mao and P. M. Bell, *Science* **191**, 851 (1976); ———, K. J. Dunn, R. M. Chrenko, R. C. Devries, *Rev. Sci. Instrum.* **50**, 1002 (1979).
48. C. M. Sung, C. Goetz, H. K. Mao, *Rev. Sci. Instrum.* **48**, 1386 (1977); C. Meade and R. Jeanloz, *Eos* **67**, 1234 (1986).
49. P. M. Bell, H. K. Mao, K. Goettel, *Science* **226**, 542 (1984); K. A. Goettel, H. K. Mao, P. M. Bell, *Rev. Sci. Instrum.* **56**, 1420 (1985).
50. J. A. Xu, H. K. Mao, P. M. Bell, *Science* **232**, 1404 (1986).
51. W. Moss, J. O. Hallquist, R. Reichlin, K. Goettel, S. Martin, *Appl. Phys. Lett.* **48**, 1256 (1986).
52. D. H. Huppert, A. Jayaraman, R. G. Maines, Sr., D. W. Steyert, P. M. Rentzepis, *J. Chem. Phys.* **81**, 5596 (1984).
53. K. Inoue, S. Akimoto, T. Ishidate, in *Solid State Physics under Pressure*, S. Minomura, Ed. (Kluwer Academic, Norwell, MA, 1985), pp. 87–92.
54. We thank the referees for constructive comments on this manuscript. Recent work performed at the Geophysical Laboratory and described above was supported by grants from the following agencies and institutions: the National Science Foundation (grants EAR-83114064, EAR-8319209, EAR-8418706), the National Aeronautics and Space Administration (grant NAGW-214), the U.S. Department of Energy (grant DE-AS05-80ER10754), and the Carnegie Institution of Washington.

# Laser Spectroscopy of Trapped Atomic Ions

WAYNE M. ITANO, J. C. BERGQUIST, D. J. WINELAND

Recent developments in laser spectroscopy of atomic ions stored in electromagnetic traps are reviewed with emphasis on techniques that appear to hold the greatest promise of attaining extremely high resolution. Among these techniques are laser cooling and the use of single, isolated ions as experimental samples. Doppler shifts and other perturbing influences can be largely eliminated. Atomic resonances with line widths of a few parts in  $10^{11}$  have been observed at frequencies ranging from the radio frequency to the ultraviolet. Experimental accuracies of one part in  $10^{18}$  appear to be attainable.

ATOMIC SPECTROSCOPY DATES FROM THE 19TH CENTURY, when it was discovered that atomic vapors emitted and absorbed light at discrete resonance wavelengths, characteristic of each chemical element. When the quantum theory of atoms was developed in the 20th century by Niels Bohr and others, it was realized that these characteristic patterns of resonances, called spectra, were due to the quantum nature of the atom. The atom normally exists only in certain states of definite energy. Transitions between these allowed states are accompanied by the absorption or emission of quanta of light, called photons. The frequency  $\nu$  of the light is related to the energy change  $\Delta E$  of the atom by the formula  $h\nu = |\Delta E|$ , where  $h$  is Planck's constant. Accurate and detailed information about atomic spectra was crucial to the development of the modern theory of quantum mechanics.

Traditional (that is, nonlaser) optical spectroscopic methods, such as dispersing the light emitted from a gas with a diffraction grating, are limited in resolution by Doppler frequency shifts. Doppler shifts are the result of the motions of the atoms in a gas and cause the

resonance absorption or emission lines to be much broader than the natural line widths (the line widths that would be observed if the atoms were motionless and isolated from perturbing influences such as collisions). Under typical laboratory conditions, the Doppler broadening results in a line width of about one millionth of the transition frequency, whereas the natural line widths are typically at least 100 times narrower. For example, the 280-nm first resonance line of  $\text{Mg}^+$ , which has a frequency of about  $1.07 \times 10^{15}$  Hz, has a Doppler-broadened line width at room temperature of about 3 GHz, whereas the natural line width is only 43 MHz. For a transition with a stable lower level, the natural line width (in hertz) is the inverse of the mean lifetime of the upper level (in seconds), divided by  $2\pi$ .

The development of tunable lasers in the 1970s led to great advances in the resolution and accuracy with which optical atomic spectra could be observed. Laser light sources have high intensity and narrow line width. These properties make it possible to use various nonlinear spectroscopic techniques, such as saturated absorption or multiphoton absorption, that cancel the effects of first-order Doppler shifts, that is, Doppler shifts that are linear in the velocities of the atoms ( $v$ ). The natural line width and the second-order Doppler shift, which is quadratic in the atomic velocities, still remain, however. The second-order Doppler shift is a result of relativistic time dilation. The atomic resonance is shifted like a clock, which runs at a rate that is slower for a moving atom than for an atom at rest. For typical laboratory conditions, this shift is very small, about one part in  $10^{12}$ . Sometimes, even this shift can be troublesome. A good example is the work of Barger *et al.* on the 657-nm transition of calcium, which has a frequency of  $4.57 \times 10^{14}$

The authors are with the Time and Frequency Division, National Bureau of Standards, Boulder, CO 80303.